Int. J. Solids Structures, 1975, Vol. 11, pp. 895–906. Pergamon Press. Printed in Great Britain.

ELASTO-DYNAMIC ANALYSIS OF RECTANGULAR PLATES WITH CIRCULAR HOLES

R. F. HEGARTY
Department of Engineering Science, Rockhurst College, Kansas City, Missouri, U.S.A.

and

T. ARIMAN
Department of Aerospace and Mechanical Engineering, University of Notre Dame, Notre Dame, IN 46556, U.S.A.

(*Received* 19 *July* 1974; *revised* 26 *December* 1974)

Abstract—The problem of the free vibrations of a rectangular elastic plate, either clamped or simply supported, with a central circular hole has been investigated by a least-squares point-matching method. The results are given in the form of curves relating the natural frequency of the plate to the hole size for a variety of Poisson's ratios. The curves do not behave monotonically, and the hole size at which the frequency is a minimum is seen to be dependent not only on the boundary conditions but also on Poisson's ratio. A two-fold mechanism of strain relief and mass reduction is proposed to explain these results as well as the results of previous studies on the vibrations of plates with discontinuities.

1. INTRODUCTION

Much attention has been given in recent years to the dynamic response of elastic plates to various types of loadings. Not surprisingly, almost all the work in this area has dealt with continuous, or complete, plates. In reality, however, most structures are flawed in some way. Portholes, welded or riveted seams, and pipe or equipment connections all constitute intentional discontinuities in the design of structures. And, if by accident, a hole or crack should appear in a plate, it would be well if the behavior of the plate in such a circumstance were known.

While a number of studies[1–25] have been done on the static behavior of plates with discontinuities, only recently the dynamic behavior of plates with cracks or holes has been considered.

The first step in the consideration of the dynamic behavior of plates is the study of the free vibrations of plates. An excellent survey of the literature in this area is given by Leissa[26], who also presents a comprehensive set of available results for the frequencies and mode shapes of free vibrations of plates. Most of these results, however, are for complete plates. Very little work has been done on the free or forced vibrations of plates with cracks or holes. Folias[27] used an integral formulation to obtain the Kirchhoff bending stresses for a plate subjected to periodic transverse vibrations and containing a through crack. Lynn and Kumbasar[28] studied the free vibrations of simply supported plates having a through line crack. They showed that the frequency equation is the eigenvalue problem of a homogeneous Fredholm integral equation of the first kind. Their work indicates that the natural frequencies of a plate decrease monotonically as the crack length increases. Stahl and Keer[29] studied the vibration and buckling problems of a plate with a through crack and showed that the solution involves homogeneous Fredholm integral equations of the second kind. They also noticed that the effect of the crack was to decrease the natural frequencies of the plate.

Unlike the problem of the vibrations of a plate with a through crack, which, if properly approached, can be handled almost exclusively by analytical techniques, the case of the free vibrations of a thin plate with a hole requires some numerical method of solution if any useful information is to be obtained. Cheng[30] was able to present a formal solution to the problem of the defraction of a plane, time-harmonic compressional wave by a group of holes in a thin plate

by the method of multiple scattering, but it appears to be of little practical use in most of the common engineering problems seen today. Kumai[31], using a numerical technique similar to that used in the present study, found the frequencies of the transverse vibrations of a square plate, with a central circular hole, and compared this numerical data with that found experimentally. Though he presented only a few graphs, a surprising trend is evident. As the hole size increases, the natural frequencies first decrease, then increase, so that for moderately large holes, the natural frequency of the plate is larger than the corresponding frequency for a complete plate. Except for presenting the data, Kumai makes no effort to explain this trend. Takahashi[32] studied the same problem by using the Rayleigh–Ritz method and deflection functions which are products of beam deflection functions. His results indicate no trend toward decreasing frequency with increasing hole size. On the contrary, the frequency increases monotonically. Figure 1 shows the general difference between the results of the previous two works.

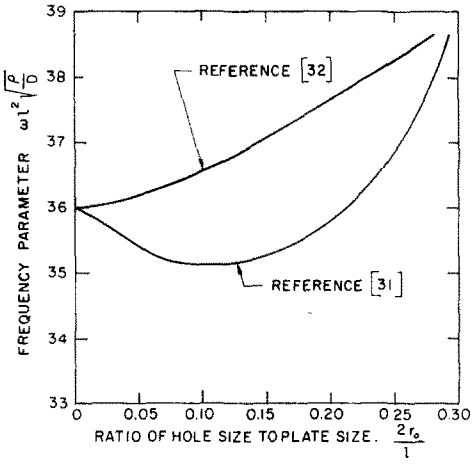

Fig. 1. Variation in frequency with hole size for a clamped plate.

The present research concerns the free vibrations of an elastic, rectangular, thin plate with a central circular hole. Results are given, in the form of curves relating frequency vs hole size, for both simply supported and clamped plates and for a variety of Poisson's ratios. The difference between Kumai's and Takahashi's studies is one reason for the present study. Another motivation arises from the authors' wish to understand more fully why two types of flawed plates behave so differently. As was previously mentioned, cracked plates exhibit a trend of decreasing frequency with increasing crack size, while plates with holes exhibit a general increase (with a possible initial decrease) of frequency with increasing hole size. It is the authors' hope that the results of this analysis help to explain, at least qualitatively, this seemingly contradictory behavior.

2. FORMULATION OF THE PROBLEM

The present research concerns the free vibrations of a thin, homogenous, isotropic, linearly elastic rectangular plate of uniform thickness h containing a central circular hole, which is free of applied stresses. One can derive from three-dimensional elasticity theory the following differential equation for plate vibrations:

$$\nabla^4 \bar{W} + \frac{\rho}{D}\frac{\partial^2 \bar{W}}{\partial t^2} = p(x, y, z, t) \tag{1}$$

where $p(x, y, z, t)$ is the external transverse load per unit area. In the case of free vibrations, $p = 0$, and equation (1) becomes:

$$\nabla^4 \bar{W} + \frac{\rho}{D}\frac{\partial^2 \bar{W}}{\partial t^2} = 0 \tag{2}$$

In equations (1) and (2), $\nabla^4 = \nabla^2\nabla^2$ is known as the biharmonic operator, ρ is the mass density, t is the time, and D is the plate flexural rigidity, defined as:

$$D = \frac{Eh^3}{12(1-\nu^2)}.$$

Here, E is Young's modulus and ν is Poisson's ratio.

If one assumes a solution of equation (2) in the form

$$\bar{W} = W\cos\omega t \tag{3}$$

where ω is the frequency of free vibration in radians per second and W is the deflection amplitude function, then equation (2) becomes:

$$\nabla^4 W = \frac{\omega^2\rho}{D} W. \tag{4}$$

3. SOLUTION OF THE PLATE PROBLEM

The solution of equation (4), as given in [26], is:

$$W = \sum_{n=0}^{\infty} \{A_nJ_n(KR) + B_nY_n(KR) + C_nI_n(KR) + D_nK_n(KR)\}\cos n\theta + \sum_{n=1}^{\infty} \{A_n^*J_n(KR) + B_n^*Y_n(KR) + C_n^*I_n(KR) + D_n^*K_n(KR)\}\sin n\theta \tag{5}$$

where $R = r/a$ is a non-dimensionalized coordinate and a has the dimensions of length. Also in (5),

$$K = ak \quad \text{where} \quad k^2 = \omega\sqrt{\frac{\rho}{D}}$$

is a frequency parameter.

In equation (5), J_n and Y_n are the Bessel functions of the first and second kinds, and I_n and K_n are modified Bessel functions of the first and second kinds, respectively. The coefficients $A_n, \ldots, D_n$ and $A_n^*, \ldots, D_n^*$ determine the mode shape and are evaluated from the boundary conditions.

The boundary conditions are: (see Fig. 2)

at $X = \pm h_1$

$$W = 0$$
$$\frac{\partial W}{\partial X} = 0 \tag{6a}$$

at $Y = \pm h_2$

$$W = 0$$
$$\frac{\partial W}{\partial Y} = 0 \tag{7a}$$

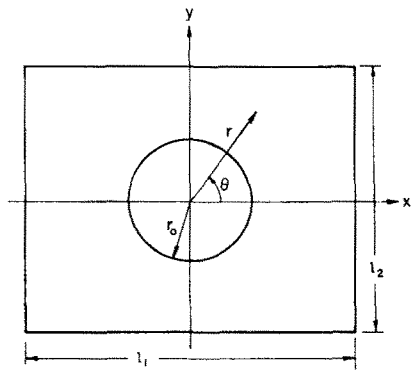

Fig. 2. Geometry of the plate.

where $X = (x/a)$ and $Y = (y/a)$. Also, $h_1 = (l_1/2a)$ and $h_2 = (l_2/2a)$. Boundary conditions (6a) and (7a) are to be used for a plate with clamped edges. If the plate is simply supported, the boundary conditions become:

at $X = \pm h_1$

$$W = 0$$
$$\frac{\partial^2 W}{\partial Y^2} = 0 \tag{6b}$$

at $Y = \pm h_2$

$$W = 0$$
$$\frac{\partial^2 W}{\partial X^2} = 0 \tag{7b}$$

where M_X and M_Y are the bending moments in the X and Y directions, respectively.

Since the circular hole is to be free of all applied stress, the boundary conditions to be satisfied along the edge of the hole are:

$$R = R_0: \qquad M_R = 0 \tag{8}$$

$$R = R_0: \qquad Q_R - \frac{1}{R}\frac{\partial M_{R\theta}}{\partial \theta} = 0 \tag{9}$$

where M_R is the bending moment normal to the edge of the hole, $M_{R\theta}$ is the twisting moment in the same plane, and Q_R is the shear force acting at the edge of the hole. Equation (9) is the familiar Kirchhoff boundary condition, which is necessary here because the fourth order system represented by equation (1) does not allow the vanishing, independently, of the shear force Q_R and the twisting moment $M_{R\theta}$.

The solution (5), along with the boundary conditions (6) through (9), uniquely determine the stress field. However, because of the rectangular boundaries, the boundary conditions cannot be satisfied identically on all the boundaries. For this reason, some numerical technique, such as least squares point-matching boundary collocation must be employed. In terms of the deflection W, equations (8) and (9) become:

$$R = R_0: \quad \frac{\partial^2 W}{\partial R^2} + \frac{\nu}{R^2}\frac{\partial^2 W}{\partial \theta^2} + \frac{\nu}{R}\frac{\partial W}{\partial R} = 0 \tag{10}$$

$$R = R_0: \quad \frac{\partial^3 W}{\partial R^3} + \frac{2-\nu}{R^2}\frac{\partial^3 W}{\partial R \partial \theta^2} - \frac{3-\nu}{R^3}\frac{\partial^2 W}{\partial \theta^2} + \frac{1}{R}\frac{\partial^2 W}{\partial R^2} - \frac{1}{R^2}\frac{\partial W}{\partial R} = 0 \tag{11}$$

Substituting the solution (5) into the boundary conditions (10) and (11), the following equations result:

$$\alpha_1 A_n + \alpha_2 B_n + \alpha_3 C_n + \alpha_4 D_n = 0 \tag{12a}$$

$$\beta_1 A_n + \beta_2 B_n + \beta_3 C_n + \beta_4 D_n = 0 \tag{12b}$$

$$\alpha_1 A_n^* + \alpha_2 B_n^* + \alpha_3 C_n^* + \alpha_4 D_n^* = 0 \tag{12c}$$

$$\beta_1 A_n^* + \beta_2 B_n^* + \beta_3 C_n^* + \beta_4 D_n^* = 0 \tag{12d}$$

where

$$\alpha_1 = J_n'' + \frac{\nu}{R_0} J_n' - \frac{\nu n^2}{R_0^2} J_n \quad \alpha_2 = Y_n'' + \frac{\nu}{R_0} Y_n' - \frac{\nu n^2}{R_0^2} Y_n$$

$$\alpha_3 = I_n'' + \frac{\nu}{R_0} I_n' - \frac{\nu n^2}{R_0^2} I_n \quad \alpha_4 = K_n'' + \frac{\nu}{R_0} K_n' - \frac{\nu n^2}{R_0^2} K_n$$

$$\beta_1 = J_n''' + \frac{1}{R_0} J_n'' - \frac{1}{R_0^2}(1 + n^2(2-\nu)) J_n' + \frac{3-\nu}{R_0^3} n^2 J_n$$

$$\beta_2 = Y_n''' + \frac{1}{R_0} Y_n'' - \frac{1}{R_0^2}(1 + n^2(2-\nu))\, Y_n' + \frac{3-\nu}{R_0^3} n^2 Y_n$$

$$\beta_3 = I_n''' + \frac{1}{R_0} I_n'' - \frac{1}{R_0^2}(1 + n^2(2-\nu))I_n' + \frac{3-\nu}{R_0^3} n^2 I_n$$

$$\beta_4 = K_n''' + \frac{1}{R_0} K_n'' - \frac{1}{R_0^2}(1 + n^2(2-\nu))K_n' + \frac{3-\nu}{R_0^3} n^2 K_n$$

A prime denotes differentiation with respect to R.

Note that the boundary conditions around the circular hole can be satisfied exactly, while the boundary conditions along the rectangular outer edges of the plate must be handled with some numerical procedure. Equations (12a) and (12b) can be solved for A_n and B_n in terms of C_n and D_n.

$$\begin{aligned} A_n &= \gamma_1 C_n + \gamma_2 D_n \\ B_n &= \gamma_3 C_n + \gamma_4 D_n \end{aligned} \tag{13}$$

where

$$\gamma_1 = \frac{\alpha_2\beta_3 - \alpha_3\beta_2}{\alpha_1\beta_2 - \alpha_2\beta_1} \qquad \gamma_2 = \frac{\alpha_2\beta_4 - \alpha_4\beta_2}{\alpha_1\beta_2 - \alpha_2\beta_1}$$

$$\gamma_3 = \frac{\alpha_3\beta_1 - \alpha_1\beta_3}{\alpha_1\beta_2 - \alpha_3\beta_1} \qquad \gamma_4 = \frac{\alpha_4\beta_1 - \alpha_1\beta_4}{\alpha_1\beta_2 - \alpha_3\beta_1}$$

Equations (12c) and (12d) show that the same relationship exists for A_n^*, B_n^*, C_n^* and D_n^*:

$$\begin{aligned} A_n^* &= \gamma_1 C_n^* + \gamma_2 D_n^* \\ B_n^* &= \gamma_3 C_n^* + \gamma_4 D_n^* \end{aligned} \tag{14}$$

Substituting the solution (5) into the boundary conditions (6) and (7), and making use of (13) and (14), the following equations result:

$$\sum_{n=0}^{\infty} \{C_n[(I_n + \gamma_1 J_n + \gamma_3 Y_n)\cos n\theta] + D_n[(K_n + \gamma_2 J_n + \gamma_4 Y_n)\cos n\theta] + C_n^*[(I_n + \gamma_1 J_n + \gamma_3 Y_n)\sin n\theta] + D_n^*[(K_n + \gamma_2 J_n + \gamma_4 Y_n)\sin n\theta]\} = 0 \tag{15}$$

Equation (15) holds at $X = \pm h_1$, $Y = \pm h_2$ for either simply supported or clamped edges.

$$\begin{aligned} \sum_{n=0}^{\infty} \Big\{ & C_n\Big[(I_n' + \gamma_1 J_n' + \gamma_3 Y_n')\cos n\theta\cos\theta + (I_n + \gamma_1 J_n + \gamma_3 Y_n)\frac{n}{R}\sin n\theta\sin\theta\Big] \\ & + D_n\Big[(K_n' + \gamma_2 J_n' + \gamma_4 Y_n')\cos n\theta\cos\theta + (K_n + \gamma_2 J_n + \gamma_4 Y_n)\frac{n}{R}\sin n\theta\sin\theta\Big] \\ & + C_n^*\Big[(I_n' + \gamma_1 J_n' + \gamma_3 Y_n')\sin n\theta\cos\theta - (I_n + \gamma_1 J_n + \gamma_3 Y_n)\frac{n}{R}\cos n\theta\sin\theta\Big] \\ & + D_n^*\Big[(K_n' + \gamma_2 J_n' + \gamma_4 Y_n')\sin n\theta\cos\theta - (K_n + \gamma_2 J_n + \gamma_4 Y_n)\frac{n}{R}\cos n\theta\sin\theta\Big]\Big\} = 0 \end{aligned} \tag{16a}$$

Equation (16a) holds at $X = \pm h_1$ for clamped edges.

$$\begin{aligned} \sum_{n=0}^{\infty} \Big\{ & C_n\Big[(\cos^2\theta + \nu\sin^2\theta)\cos n\theta(I_n'' + \gamma_1 J_n'' + \gamma_3 Y_n'') + \frac{1}{R}(2n(1-\nu)\sin\theta\cos\theta\sin n\theta \\ & + \cos n\theta(\sin^2\theta + \nu\cos^2\theta))(I_n' + \gamma_1 J_n' + \gamma_3 Y_n') - \frac{n}{R^2}(n\cos n\theta(\sin^2\theta + \nu\cos^2\theta) \\ & + 2(1-\nu)\sin\theta\cos\theta\sin n\theta)(I_n + \gamma_1 J_n + \gamma_3 Y_n)\Big] \\ & + D_n\Big[\cos n\theta(\cos^2\theta + \nu\sin^2\theta)(K_n'' + \gamma_2 J_n'' + \gamma_4 Y_n'') + \frac{1}{R}(2n(1-\nu)\sin\theta\cos\theta\sin n\theta \\ & + \cos n\theta(\sin^2\theta + \nu\cos^2\theta))(K_n' + \gamma_2 J_n' + \gamma_4 Y_n') - \frac{n}{R^2}(n\cos n\theta(\sin^2\theta + \nu\cos^2\theta) \end{aligned}$$

$$+2(1-\nu)\sin\theta\cos\theta\sin n\theta)(K_n+\gamma_2 J_n+\gamma_4 Y_n)\Big]$$

$$+C_n^*\Big[\sin n\theta(\cos^2\theta+\nu\sin^2\theta)(I_n''+\gamma_1 J_n''+\gamma_3 Y_n'')+\frac{1}{R}(\sin n\theta(\sin^2\theta+\nu\cos^2\theta)$$

$$-2n(1-\nu)\sin\theta\cos\theta\cos n\theta)(I_n'+\gamma_1 J_n'+\gamma_3 Y_n')+\frac{n}{R_2}(2(1-\nu)\sin\theta\cos\theta\cos n\theta$$

$$-n\sin\theta(\sin^2\theta+\nu\cos^2\theta))(I_n+\gamma_1 J_n+\gamma_3 Y_n)\Big]$$

$$+D_n^*\Big[\sin n\theta(\cos^2\theta+\nu\sin^2\theta)(K_n''+\gamma_2 J_n''+\gamma_4 Y_n'')+\frac{1}{R}(\sin n\theta(\sin^2\theta+\nu\cos^2\theta)$$

$$-2n(1-\nu)\sin\theta\cos\theta\cos n\theta)(K_n'+\gamma_2 J_n'+\gamma_4 Y_n')+\frac{n}{R^2}(2(1-\nu)\sin\theta\cos\theta\cos n\theta$$

$$-n\sin\theta(\sin^2\theta+\nu\cos^2\theta))(K_n+\gamma_2 J_n+\gamma_4 Y_n)\Big]\Big\}=0 \tag{16b}$$

Equation (16b) holds at $X=\pm h_1$ for simply supported edges.

$$\sum_{n=0}^{\infty}\Big\{C_n\Big[(I_n'+\gamma_1 J_n'+\gamma_3 Y_n')\cos n\theta\sin\theta+\frac{n}{R}(I_n+\gamma_1 J_n+\gamma_3 Y_n)\sin n\theta\cos\theta\Big]$$

$$+D_n\Big[(K_n'+\gamma_2 J_n'+\gamma_4 Y_n')\cos n\theta\sin\theta-\frac{n}{R}(K_n+\gamma_2 J_n+\gamma_4 Y_n)\sin n\theta\cos\theta\Big]$$

$$+C_n^*\Big[(I_n'+\gamma_1 J_n'+\gamma_3 Y_n')\sin n\theta\sin\theta+\frac{n}{R}(I_n+\gamma_1 J_n+\gamma_3 Y_n)\cos n\theta\cos\theta\Big]$$

$$+D_n^*\Big[(K_n'+\gamma_2 J_n'+\gamma_4 Y_n')\sin n\theta\sin\theta+\frac{n}{R}(K_n+\gamma_2 J_n+\gamma_4 Y_n)\cos n\theta\cos\theta\Big]\Big\}=0 \tag{17a}$$

Equation (17a) holds at $Y=\pm h_2$ for clamped edges.

$$\sum_{n=0}^{\infty}\Big\{C_n\Big[\cos n\theta(\sin^2\theta+\nu\cos^2\theta)(I_n''+\gamma_1 J_n''+\gamma_3 Y_n'')+\frac{1}{R}(\cos n\theta(\cos^2\theta+\nu\sin^2\theta)$$

$$-2n(1-\nu)\sin\theta\cos\theta\sin n\theta)(I_n'+\gamma_1 J_n'+\gamma_3 Y_n')-\frac{n}{R^2}(n\cos n\theta(\cos^2\theta+\nu\sin^2\theta)$$

$$-2(1-\nu)\sin\theta\cos\theta\sin n\theta)(I_n+\gamma_1 J_n+\gamma_3 Y_n)\Big]$$

$$+D_n\Big[\cos n\theta(\sin^2\theta+\nu\cos^2\theta)(K_n''+\gamma_2 J_n''+\gamma_4 Y_n'')+\frac{1}{R}(\cos n\theta(\cos^2\theta+\nu\sin^2\theta)$$

$$-2n(1-\nu)\sin\theta\cos\theta\sin n\theta)(K_n'+\gamma_2 J_n'+\gamma_4 Y_n')-\frac{n}{R^2}(n\cos n\theta(\cos^2\theta+\nu\sin^2\theta)$$

$$-2(1-\nu)\sin\theta\cos\theta\sin n\theta)(K_n+\gamma_2 J_n+\gamma_4 Y_n)\Big]$$

$$+C_n^*\Big[\sin n\theta(\sin^2\theta+\nu\cos^2\theta)(I_n''+\gamma_1 J_n''+\gamma_3 Y_n'')+\frac{1}{R}(\sin n\theta(\cos^2\theta+\nu\sin^2\theta)$$

$$+2n(1-\nu)\sin\theta\cos\theta\cos n\theta)(I_n'+\gamma_1 J_n'+\gamma_3 Y_n')-\frac{n}{R^2}(n\sin n\theta(\cos^2\theta+\nu\sin^2\theta)$$

$$+2(1-\nu)\sin\theta\cos\theta\cos n\theta)(I_n+\gamma_1 J_n+\gamma_3 Y_n)\Big]$$

$$+D_n^*\Big[\sin n\theta(\sin^2\theta+\nu\cos^2\theta)(K_n''+\gamma_2 J_n''+\gamma_4 Y_n'')+\frac{1}{R}(\sin n\theta(\cos^2\theta+\nu\sin^2\theta)$$

$$+2n(1-\nu)\sin\theta\cos\theta\cos n\theta)(K_n'+\gamma_2 J_n'+\gamma_4 Y_n')-\frac{n}{R^2}(n\sin n\theta(\cos^2\theta+\nu\sin^2\theta)$$

$$+2(1-\nu)\sin\theta\cos\theta\cos n\theta)(K_n+\gamma_2 J_n+\gamma_4 Y_n)\Big]\Big\}=0 \tag{17b}$$

Equation (17b) holds at $Y=\pm h_2$ for simply supported edges. The original vector of $8n+4$ unknowns $[A_n, B_n, C_n, D_n, A_n^*, B_n^*, C_n^*, D_n^*]$ has now been reduced to the vector of $4n+2$ unknowns $[C_n, D_n, C_n^*, D_n^*]$, which now must be determined from equations (15–17).

Since the rectangular boundaries are not coordinate lines, an exact solution of equations (15–17) cannot be found. To obtain an approximate solution, the infinite series solution (5) is truncated at $n = N$, leaving $4N + 2$ unknowns to be determined. M points are chosen along the plate outer boundaries, and since there are two conditions for each point, $2M$ equations are generated. For $2M = 4N + 2$, the equations can be solved for the unknowns. However, if $2M > 4N + 2$, and the unknowns are determined in the least squares sense, then, as $M \to \infty$, this process becomes that of minimizing the integral of the squared error.

The set of equations which result from satisfying the boundary conditions at M points can be written in matrix form:

$$\mathbf{A}[C_n, D_n, C_n^*, D_n^*] = 0$$

where $\mathbf{A}$ is a $2M$ by $4N + 2$ matrix whose coefficients are functions of the frequency ω, and $[Cn, D_n, C_n^*, D_n^*]$ is the $4N + 2$ vector of unknowns. It is shown in Ref. [9] that a necessary condition that the vector of unknowns minimize the squared error is that the unknowns satisfy

$$\mathbf{A}^T\mathbf{A}[C_n, D_n, C_n^*, D_n^*] = 0 \tag{18}$$

where $\mathbf{A}^T$ is the transpose of $\mathbf{A}$ and $\mathbf{A}^T\mathbf{A}$ is a $4N + 2$ by $4N + 2$ square matrix. For equation (18) to have a nontrivial solution, the determinant of $\mathbf{A}^T\mathbf{A}$ must vanish. Therefore:

$$|\mathbf{A}^T\mathbf{A}| = 0 \tag{19}$$

Equation (19) is the frequency equation which can now be solved to obtain the natural frequencies of the plate.

4. RESULTS AND DISCUSSION

As was stated above, equation (19) is the frequency equation which, when solved, will yield the natural frequencies of the plate. Results will now be presented for a square plate, both simply supported and clamped, for a variety of Poisson's ratios. Thus, $l_1 = l_2 = l$ (or $h_1 = h_2$). The infinite series solution (5) is truncated at $n = 4$, leaving eighteen unknowns to be determined. Sixteen points along the outer boundaries of the plate are chosen ($M = 16$), yielding thirty-two equations in the eighteen unknowns. Thus, equation (19) is a determinantal equation of order eighteen, and the values of ω which cause the determinant to vanish are the natural frequencies of the plate.

It was noted by Hoffman and Ariman [9] that the best accuracy in the least-squares point-matching technique was obtained when the ratio of equations to unknowns was about 2 in the rectangular plate problem with a circular hole. For the verification of this conclusion, the case of a simply-supported square plate with no hole was considered. A closed-form solution for this problem exists, but the natural frequency was sought by the point-matching method so that a measure of accuracy could be obtained. Holding the number of collocation points constant, it was found that truncating the solution at $n = 4$ gave the best results from the standpoint of accuracy and computational difficulty. With $n = 4$ the number of collocation points was varied between 8 and 40 and it was found that 16 collocation points yielded the most accurate estimate of the natural frequency. For this case the natural frequency resulting from these equations differed from the result of the closed-form solution by less than 1 per cent. It should also be noted that Kumai's solution [31] differs from the present one in that the functional form of his solution for a square plate contains only cosine terms, whereas the present solution (equation 5) for a rectangular plate imposes no symmetry restriction in θ and thereby both sine and cosine terms are retained.

Obviously, some numerical technique is needed to solve equation (19), and it was decided to use Muller's iterative technique [33], which is a quadratic interpolation scheme for finding the roots of an equation. This technique requires the evaluation of the determinant at three trial values of ω, and then uses these values to generate the next estimate. If the first three estimates are reasonably good (i.e. to within 10 per cent), only five to ten iterations are required to determine the frequency.

In the introduction, two reasons were given for the present study. First, Kumai [31], utilizing a technique similar to the one employed here, noticed an initial decrease in frequency with increasing hole size, after which the frequency increased. Takahashi [32], on the other hand, noticed no such

trend. Both works were done for a Poisson's ratio of 0.3. Takahashi used the Rayleigh-Ritz method and beam deflection functions. His results indicate only an increase in frequency with increasing hole size.

The curves given in Figs. 3 and 4 show some of the results of the present study. Figure 3 shows the variation of the frequency parameter:

$$\omega^* = \omega l^2 \sqrt{\frac{\rho}{D}}$$

with increasing hole size for a simply supported plate, while Fig. 4 shows the same study for a clamped plate. For a plate with no hole, the frequency parameter $\omega^* = 19.739$ for a simply supported plate and $\omega^* = 35.984$ for a clamped plate. The numerical technique used here yields results to within one per cent of these values. In Fig. 4 a comparison of the Takahashi's results [31] with those of the present study for a Poisson's ratio of 0.3 is also presented. Greater difference is observed for smaller holes.

As Figs. 3 and 4 show, there is indeed an initial decrease in frequency with increasing hole size,

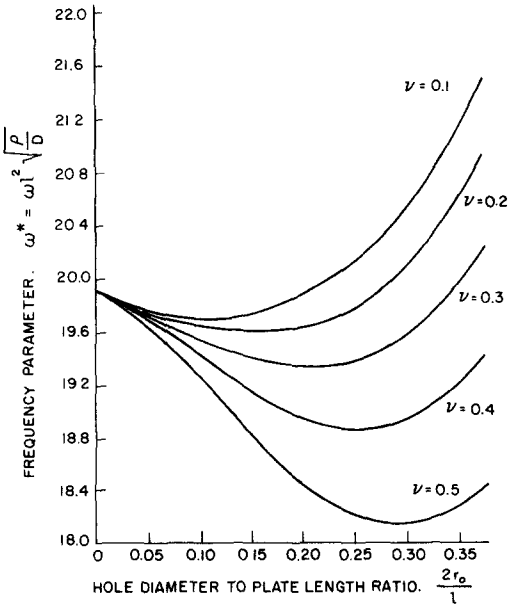

Fig. 3. Variation in frequency with hole size for a simply supported, square plate.

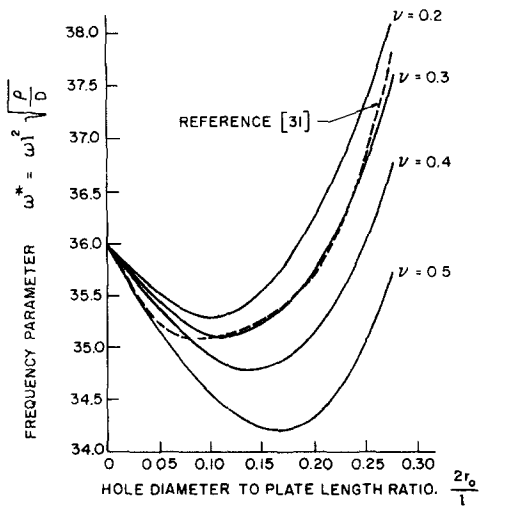

Fig. 4. Variation in frequency with hole size for a clamped, square plate.

the extent of this decrease depending on Poisson's ratio. It should be noted that the frequency parameter ω^* used in Figs. 3 and 4 is itself a function of ν.

Thus, two points on different curves but on the same horizontal line have the same frequency parameter ω^*; however, their frequencies are not equal. To better illustrate the effect of hole size and Poisson's ratio on the frequency ω, Figs. 5 and 6 show the variation in frequency with hole size. The frequency parameter used in these figures is independent of ν. It might be noted that the larger frequencies belong to the plate with the larger Poisson's ratio. This is in keeping with the fact that, other things being equal, the plate with the greater strain energy will have the higher frequency. As Poisson's ratio increases, the lateral strain energy increases, and thus, the total potential energy of the system increases.

As was stated, Figs. 3 and 4 indicate that Kumai's[31] analysis was more accurate than Takahashi's[32]. However, a closer look at these figures show that the tendency of the frequency to decrease is greatly affected by Poisson's ratio. If the hole diameter to plate length ratio $2r_0/l$ at which the frequency is a minimum is called the critical ratio R_c, then it is clear from the figures that R_c decreases as Poisson's ratio decreases. Table 1 and Fig. 7 show this trend explicitly.

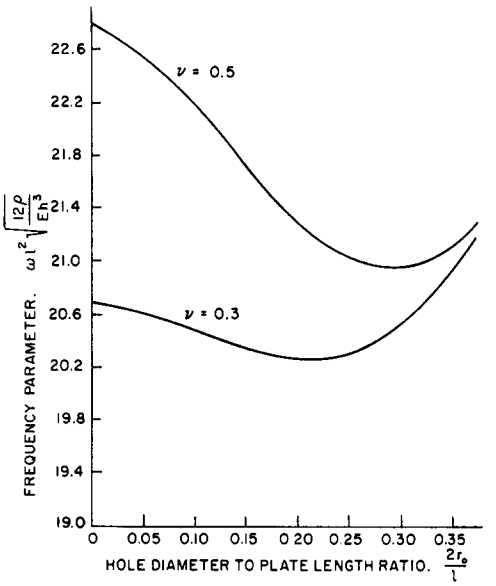

Fig. 5. Variation in frequency with hole size for a simply supported, square plate. The frequency parameter is independent of Poisson's ratio.

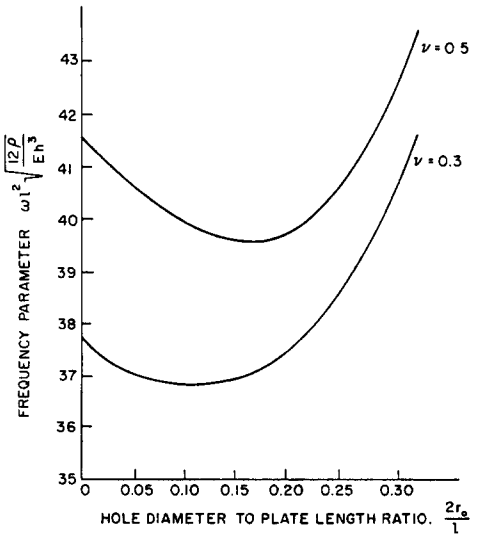

Fig. 6. Variation in frequency with hole size for a clamped square plate. The frequency parameter is independent of Poisson's ratio.

Table 1. Variation in critical hole ratio with Poisson's ratio

ν	R_c'	R_c''
.10	.1000	-----*
.15	.1375	.0625
.20	.1625	.0875
.25	.1875	.1000
.30	.2125	.1125
.35	.2375	.1250
.40	.2625	.1375
.45	.2750	.1500
.50	.2875	.1625

R_c' is the critical hole ratio for a simply supported plate

R_c'' is the critical hole ratio for a clamped plate

$$R_c = \left(\frac{2r_o}{l}\right)_c$$

* No value of R_c'' was found for $\nu = .10$ because for a clamped plate the numerical solution becomes unstable at hole ratios less than .1.

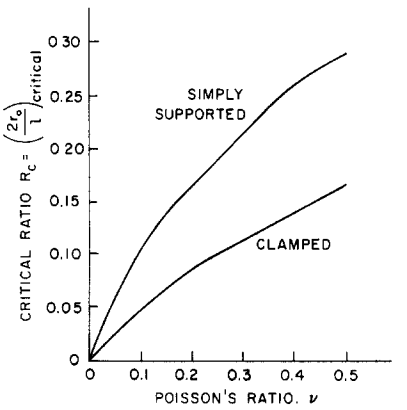

Fig. 7. Variation in critical hole ratio with Poisson's ratio for both clamped and simply supported plates.

It appears from Fig. 7 that, at $\nu = 0$, the critical ratio R_c is either zero or very small. Thus, the present analysis can reproduce Takahashi's results if ν is set equal to zero. In reality however, it appears that Takahashi's analysis had the effect of setting $\nu = 0$. Recall that Takahashi, in using the Rayleigh-Ritz method, employed as his comparison functions a set of functions derived from beam deflection functions. Such functions approximate plate functions fairly well, except for the fact that elementary beam theory allows free lateral contraction and expansion (i.e. $\nu = 0$). Thus, Takahashi was in effect replacing his plate with an infinite number of beams, and, in so doing, setting Poisson's ratio, for his study, equal to zero. The curve representing Takahashi's work, given in Fig. 1, and yielding $R_c = 0$, is actually an asymptotic curve for the set of curves in Figs. 3 and 4.

One other motivation for the present study was mentioned in the introduction. It was noted there that, in two studies on the free vibrations of cracked plates [28, 29], the natural frequency decreased as crack size increased, as opposed to the behaviour of a plate with a hole, shown in Figs. 3–6. It was hoped that this study could explain, at least qualitatively, the reason for this difference.

It was mentioned earlier in this study that the effect of an increase in Poisson's ratio was an increase in the lateral strain energy of the plate. This of course increases the total potential energy of the plate and thus increases the frequency. Likewise, any mechanism that tends to decrease the lateral strain energy will cause a decrease in the frequency of the plate. A through crack is such a mechanism. Along its free edges, the plate material is allowed to expand and contract freely. Thus, the crack behaves as a strain reliever. As the crack gets longer, more free surface is available to relieve lateral strain, and thus the total energy (and the frequency) of the plate decreases. This would explain the behavior of cracked plates noted in [28, 29].

A hole in the plate would reduce lateral strain energy in the same way as a crack does. The

presence of the hole, however, introduces another effect. Just as a reduction in energy will reduce the frequency of a system, the reduction of its mass will tend to increase it. For a thin crack, the mass reduction is negligible, but for a hole, it can easily be the dominant effect. Since strain relief depends on the free surface available, the effect of the reduction of lateral strain energy by a hole would increase, more or less, as the diameter of the hole. However, the effect of mass reduction, which tends to increase the frequency of the plate, would increase as the square of the diameter of the hole. Thus, for a small hole, the reduction of strain might well be the dominant influence, and the frequency would decrease. However, it would appear that as the hole gets larger, the effect of mass reduction would soon replace strain relief as the primary factor, and the frequency would begin to increase. Figure 8 shows an attempt to give some quantitative backing to this explanation of the

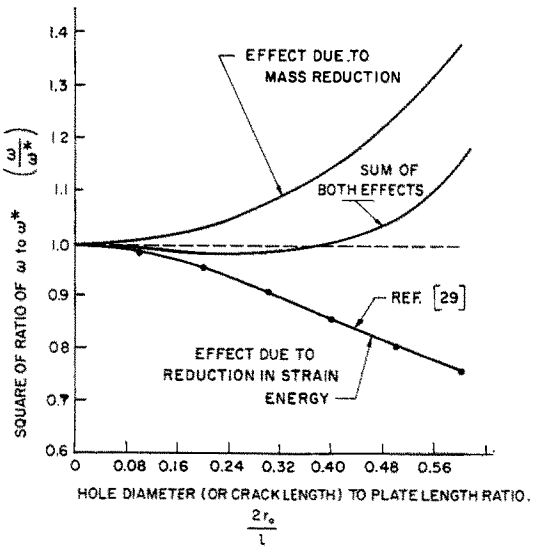

Fig. 8. Illustrations of mechanisms for strain energy reduction and mass reduction effects on frequency of plate.

curves of Figs. 3–6. The top curve in Fig. 8 represents the effect of mass reduction alone on the frequency ω of a plate. If all other quantities are kept constant, the frequency ω of the plate is given by

$$\omega = \frac{\text{constant}}{\sqrt{\text{mass}}}.$$

Of course, reducing the mass of a plate by cutting a hole in the center is not the same as uniformly reducing the density of the plate, but the above formula at least provides something to work with. The bottom curve in Fig. 8 represents the results of the work of Stahl and Keer[29], who studied free vibrations of a simply supported, cracked plate with a Poisson's ratio of 0.3. It is assumed here that this curve represents only the effect of strain relief on the frequency of a plate. The middle curve is the sum of the other two. Three things should be noted about this curve. First, it has the general shape of the curves in Figs. 3–6. Also, R_c for this curve is approximately equal to R_c from the curve for $\nu = 0.3$ in Fig. 3. Lastly, the frequency corresponding to R_c from this curve is about one percent higher than the value from Fig. 3.

The interaction between strain relief and mass reduction can also explain the variation of R_c with Poisson's ratio, shown in Fig. 7. As ν decreased, the contribution of the lateral strain energy to the total potential energy of the plate also decreases. Thus, the effect of strain relief is not as important in plates with small ν as it is for plates with large ν. If a plate has little strain energy to begin with, the effect of mass reduction can more easily become dominant, causing R_c to have a small value. Conversely, if a large part of the total energy is composed of lateral strain energy, as it is in plates with large ν, it would be expected that the effect of strain energy reduction would dominate over a large range of hole sizes. Considering all this, it is not surprising that R_c decreases with ν.

Acknowledgements—The content of this paper is a part of a dissertation[34] by the first author submitted to the Graduate School of the University of Notre Dame in partial fulfillment of the requirements for the degree of Doctor of Philosophy. This work was supported by the Department of the Navy, under Deep Sea Engineering Project and Contract ONR-N00014-68-A-0152 to the University of Notre Dame. The authors also acknowledge the valuable suggestions of the reviewers.

REFERENCES

1. D. D. Ang and M. L. Williams, Combined stresses in an orthotropic plate having a finite crack. *J. Appl. Mech. Trans. of ASME* **28**, 372 (1961).
2. R. Bailey and R. Hicks, Behavior of perforated plates under plane stress. *J. Mech. Engng Sci.* **2**, 2, 143 (1960).
3. A. M. Averin, On the bending of a cantilever plate weakened by a hole of arbitrary shape. *Theory of Plates and Shells.* NASA TT. F-341 TT66-51021, 142 (1962).
4. A. Baratov, Study of the stability of elastic rectangular plates with a rectangular hole, built-in by the outer and inner contours. *Theory of Plates and Shells.* NASA TT F-341 TT66-51021, 193 (1962).
5. F. Erdogan, The stress distribution in an infinite plate with two collinear cracks subject to arbitrary loads in plane. *Proc. 4th U. S. Nat. Cong. Appl. Mech.* 547 (1962).
6. A. F. Emery and C. M. Segedin, The evaluation of the stress intensity factors for cracks subjected to tension, torsion, and flexure by an efficient numerical technique. *J. Basic Engng. Transactions of ASME*, **94**, 387 (1972).
7. M. I. Dlugach and A. I. Shinkar, Use of digital computers in the calculation of smooth and ribbed plates and shells, either not stressed or stressed by holes. *Theory of Plates and Shells.* NASA TT. F-341 TT66-51021, 402 (1962).
8. A. J. Durelli, V. J. Parks and H. C. Feng, Stresses around an elliptical hole in a finite plate subjected to axial loading, *J. Appl. Mech. Transactions of ASME* **33**, 192 (1966).
9. R. E. Hoffman and T. Ariman, Thermal bending of plates with circular holes. *Nucl. Engng Design* **14**, 231 (1970).
10. G. R. Irwin, Analysis of stresses and strains near the end of a crack traversing a plate. *J. Appl. Mech. Transactions of ASME*, **24**, 361 (1957).
11. J. K. Knowles and N. M. Wang, On the bending of an elastic plate containing a crack, *J. Math. Phys.* **39**, 223 (1960).
12. L. M. Keer and C. Sve, On the bending of cracked plates, *Int. J. Solids Structures* **6**, 1545 (1970).
13. I. Y. Khoma, Stress concentration in a thin plate weakened by an infinite number of circular holes under elastic-plastic strains. *Theory of Plates and Shells.* NASA TT F-341 TT66-51021, 888 (1962).
14. N. Jones, and D. Hozos, A study of the stresses around elliptical holes in flat plates. *J. Engng for Industry, Transactions of ASME* **93**, 688 (1971).
15. Y. N. Muzychenko, Bending and stability of rectangular plates weakened by rectangular cuts. *Theory of Plates and Shells.* NASA TT F-341 TT66-51021, 667 (1962).
16. K. S. Rao, M. N. B. Rao and T. Ariman, Thermal stresses in plates with circular holes. *Nucl. Engng Design* **15**, 97 (1971).
17. K. S. Rao, M. N. B. Rao and T. Ariman, Thermal stresses in elastic plates with elliptic holes. ASME *J. Engng for Industry* Paper No. 73-WA/DE-3, (1974).
18. C. C. Lo and A. W. Leissa, Bending of plates with circular holes. *Acta Mech.* **1**, 64 (1967).
19. C. B. Ling, On the stresses in a plate containing two circular holes. *J. Appl. Phys.* **19**, 77 (1948).
20. G. N. Savin, Concentration stresses around curvilinear holes in plates and shells. *Proc. 11th Int. Cong. Appl. Mech.* (Edited by H. Görther) Munich, 289 (1964).
21. I. A. Tsurpal, Study of the stressed and strained state of a physically nonlinearly elastic plate with reinforced circular hole. *Theory of Plates and Shells.* NASA TT F-341 TT66-51021, 899 (1962).
22. W. K. Wilson, Numerical method for determining stress intensity factors of an interior crack in a finite plate. *J. Basic Engng Transactions of ASME* **93**, 685 (1971).
23. M. L. Williams, The bending stress distribution at the base of a stationary crack. *J. Appl. Mech. Transactions of ASME* **28**, 78 (1961).
24. M. L. Williams, On the stress distribution at the base of a stationary crack. *J. Appl. Mech. Transactions of ASME* **24**, 109 (1957).
25. M. L. Williams, Surface stress singularities resulting from various boundary conditions in angular corners of plates under bending. *Proc. 1st U. S. Nat. Cong. Appl. Mech.* 325 (1950).
26. A. W. Leissa, *Vibrations of Plates.* NASA SP-160 (1969).
27. E. S. Folias, On the steady-state transverse vibrations of a cracked plate. *Engng Fract. Mech.* **1**, 363 (1968).
28. P. P. Lynn and N. Kumbasar, Free vibrations of thin rectangular plates having narrow cracks with simply supported edges. *Developments in Mechanics* **4**, Proceedings of the Tenth Midwestern Mechanics Conference, 911 (1967).
29. B. Stahl and L. M. Keer, Vibration and stability of cracked rectangular plates. *Int. J. Solids Structures* **8**, 69 (1972).
30. S. L. Cheng, Dynamic stresses in a plate with circular holes. *J. Appl. Mech. Transactions of ASME* **39**, 129 (1972).
31. T. Kumai, Flexural vibration of the square plate with a central circular hole. *Proc. 2nd Japan Nat. Cong. Appl. Mech.* (1952).
32. S. Takahashi, Vibration of rectangular plates with circular holes. *Bulletin of JSME*, **1**, 4 (1958).
33. S. D. Conte, *Elementary Numerical Analysis.* McGraw-Hill, New York (1965).
34. R. F. Hegarty, Dynamic Analysis of Cracked Cylindrical Shells and Plates with Holes. Ph.D. Thesis submitted to the University of Notre Dame (1973). Also T. Ariman and R. F. Hegarty, *Nucl. Engng Design* **29**, 89 (1974).